Nonlinear Dyn
DOI 10.1007/s11071-010-9780-9

ORIGINAL PAPER

Analytics of heteroclinic bifurcation in a 3:1 subharmonic resonance

Mohamed Belhaq · Abdelhak Fahsi

Received: 8 April 2010 / Accepted: 6 July 2010

Abstract Analytical approximation of heteroclinic bifurcation in a 3:1 subharmonic resonance is given in this paper. The system we consider that produces this bifurcation is a harmonically forced and self-excited nonlinear oscillator. This bifurcation mechanism, resulting from the disappearance of a stable slow flow limit cycle at the bifurcation point, gives rise to a synchronization phenomenon near the 3:1 resonance. The analytical approach used in this study is based on the collision criterion between the slow flow limit cycle and the three saddles involved in the bifurcation. The amplitudes of the 3:1 subharmonic response and of the slow flow limit cycle are approximated and the collision criterion is applied leading to an explicit analytical condition of heteroclinic connection. Numerical simulations are performed and compared to the analytical finding for validation.

Keywords Heteroclinic bifurcation · 3:1 subharmonic resonance · Frequency-locking · Perturbation analysis · Double reduction technique

M. Belhaq (✉)
Laboratory of Mechanics, University Hassan II-Casablanca, Casablanca, Morocco
e-mail: mbelhaq@yahoo.fr

A. Fahsi
FSTM, University Hassan II-Mohammadia, Mohammadia, Morocco

1 Introduction

In this work, we give an analytical approximation of heteroclinic bifurcation to a stable slow flow limit cycle near the 3:1 subharmonic resonance in a forced van der Pol–Duffing oscillator. This bifurcation takes place when pairs of saddles form three connections destroying a limit cycle and giving rise to synchronization between the limit cycle and the subharmonic response in which the response of the system follows the 3:1 subharmonic frequency.

To approximate heteroclinic connection, numerical simulations are usually used. For instance, a heteroclinic bifurcation near a 4:1 resonance has been analyzed in a nonlinear parametric oscillator using the fourth-order Runge–Kutta method [1, 2]. Later, a Ph.D. thesis [3] has been devoted to investigate this 4:1 resonance problem using continuation methods. Recently, an extensive and a detailed numerical path-following and simulation was carried out to analyze bifurcation to heteroclinic cycles in three and four coupled phase oscillators [4]. Note that bifurcation to heteroclinic cycles are of great interest because of their applications in synchronization phenomena in many fields in physics and biology [5–7]. While heteroclinic bifurcations for cycles have been studied extensively from numerical view point, analytical approximations of these bifurcations in periodically forced nonlinear oscillators remains to be explored.

In this paper, we propose an analytical treatment of heteroclinic bifurcation of cycles near the 3:1 res-

Published online: 04 August 2010

onance. This is done by using the so-called collision criterion based on the coalescence, at the bifurcation, between the slow flow limit cycle and the three saddles involved in the bifurcation. This criterion was widely applied in a series of a paper [8–12] to capture homoclinic and heteroclinic bifurcations in two- and three-dimensional autonomous systems. It was shown that the collision criterion is equivalent to the Melnikov method [10]; the collision criterion is accessible via approximations of limit cycles, the Melnikov approach, on the other hand, aims directly at the separatrices. Moreover, it was concluded that the application of the collision criterion gives a satisfactory approximation when using trigonometric functions in approximating the limit cycle, whereas the criterion coincides with the Melnikov method when using the Jacobian elliptic functions [8–10]. It should be emphasized that the collision criterion was also applied to formally derive an analytical approximation of homoclinic bifurcation in three-dimensional systems [11, 12].

The rest of the paper is organized as follows: In Sect. 2 we use, in a first step, the multiple scales method to derive the slow flow and the amplitude-frequency response near the 3:1 subharmonic resonance. Then, a multiple scales method is performed, in a second step, on the slow flow to approximate the limit cycle. In Sect. 3, we investigate the heteroclinic bifurcation using the collision criterion and we compare the analytical finding with the numerical simulations obtained by examining the phase portraits. Section 4 concludes the work.

2 3:1 Subharmonic response and slow flow limit cycle

The system we consider that exhibits a 3:1 heteroclinic connection is a forced van der Pol–Duffing oscillator given in the dimensionless form as

$$\ddot{x} + \omega_0^2 x - \left(\alpha - \beta x^2\right)\dot{x} - \gamma x^3 = h\cos\omega t \tag{1}$$

where ω_0 is the natural frequency, α, β are the damping coefficients, γ is the nonlinear component and h, ω are the amplitude and the frequency of the external excitation, respectively. The purpose is to approximate the amplitude-frequency response of the 3:1 resonance as well as the slow flow limit cycle of (1). Thus, the 3:1 resonance condition is expressed by introducing a detuning parameter σ according to

$$\omega_0^2 = \left(\frac{\omega}{3}\right)^2 + \sigma \tag{2}$$

and we use the method of multiple scales [19]. Introducing a book-keeping parameter ε in (1) and (2), we obtain

$$\ddot{x} + \left(\frac{\omega}{3}\right)^2 x = h\cos\omega t + \varepsilon\left\{-\sigma x + (\alpha - \beta x^2)\dot{x} + \gamma x^3\right\} \tag{3}$$

We seek a two-scale expansion of the solution in the form

$$x(t) = x_0(T_0, T_1) + \varepsilon x_1(T_0, T_1) + O\left(\varepsilon^2\right) \tag{4}$$

where $T_i = \varepsilon^i t$. Substituting (4) into (3) and equating coefficients of the same power of ε, we obtain the following set of linear partial differential equations

$$D_0^2 x_0(T_0, T_1) + \left(\frac{\omega}{3}\right)^2 x_0(T_0, T_1) = h\cos\omega T_0 \tag{5}$$

$$\begin{aligned} &D_0^2 x_1(T_0, T_1) + \left(\frac{\omega}{3}\right)^2 x_1(T_0, T_1) \\ &\quad = -2D_0 D_1 x_0 - \sigma x_0 + \left(\alpha - \beta x_0^2\right) D_0 x_0 + \gamma x_0^3 \end{aligned} \tag{6}$$

where $D_i^j = \frac{\partial^j}{\partial T_i^j}$. The solution to the first order is given by

$$x_0(T_0, T_1) = r(T_1)\cos\left(\frac{\omega}{3}T_0 + \theta(T_1)\right) + F\cos\omega T_0 \tag{7}$$

where r and θ are, respectively, the amplitude and the phase of the response and $F = -\frac{9h}{8\omega^2}$. Substituting (7) into (6), removing secular terms and using the expressions $\frac{dr}{dt} = \varepsilon D_1 r + O(\varepsilon^2)$ and $\frac{d\theta}{dt} = \varepsilon D_1\theta + O(\varepsilon^2)$, we obtain the slow flow modulation equations of amplitude and phase

$$\begin{aligned} \frac{dr}{dt} &= Ar - Br^3 - (H_1\sin 3\theta + H_2\cos 3\theta)r^2, \\ \frac{d\theta}{dt} &= S - Cr^2 - (H_1\cos 3\theta - H_2\sin 3\theta)r \end{aligned} \tag{8}$$

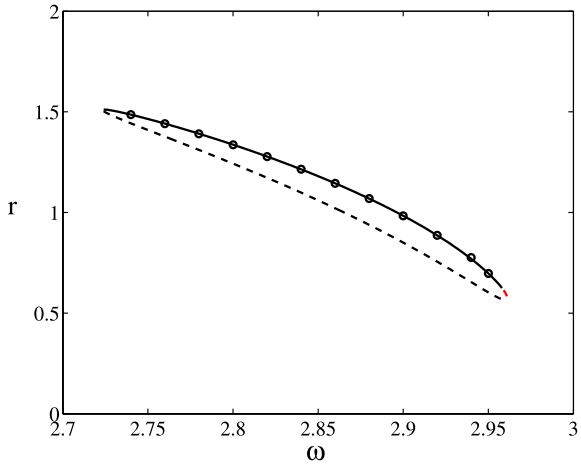

Fig. 1 Amplitude–frequency response curve near 3:1 resonance. *Solid line* for stable, *dashed line* for unstable and *circles* for numerical simulation, $\alpha = 0.01$, $\beta = 0.05$, $\gamma = 0.1$, $h = 1$

where $A = \frac{\alpha}{2} - \frac{\beta F^2}{4}$, $B = \frac{\beta}{8}$, $C = \frac{9\xi}{8\omega}$, $S = \frac{3\sigma}{2\omega} - \frac{9\xi F^2}{4\omega}$, $H_1 = \frac{9\xi F}{8\omega}$, and $H_2 = \frac{\beta F}{8}$. Equilibria of the slow flow (8), corresponding to periodic solutions of (1), are determined by setting $\frac{dr}{dt} = \frac{d\theta}{dt} = 0$. This leads to the amplitude–frequency response equation

$$A_2 r^4 + A_1 r^2 + A_0 = 0 \tag{9}$$

and the phase–frequency response relation

$$\tan 3\theta = \frac{(A - Br^2)H_1 - (S - Cr^2)H_2}{(A - Br^2)H_2 + (S - Cr^2)H_1} \tag{10}$$

where $A_2 = B^2 + C^2$, $A_1 = -(2AB + 2SC + H_1^2 + H_2^2)$ and $A_0 = A^2 + S^2$.
Figure 1 shows the variation of the amplitude–frequency response curve, as given by (9), for the given parameters $\alpha = 0.01$, $\beta = 0.05$, $\gamma = 0.1$ and $h = 1$. The solid line denotes a stable branch and the dashed line denotes an unstable one. The stability analysis has been done using the Jacobian of the slow flow system (8). Results from numerical simulation (circles) using Runge–Kutta method are also plotted for validation. For extensive numerical simulations, see [13, 14].

To approximate the slow flow limit cycle, corresponding to quasiperiodic solution of (1), we introduce a new small book-keeping parameter μ to perform a second perturbation analysis on the following slow flow Cartesian system corresponding to the polar form (8)

$$\begin{aligned}
\frac{du}{dt} &= Sv + \mu\big\{Au - (Bu + Cv)\big(u^2 + v^2\big) \\
&\quad + 2H_1 uv - H_2\big(u^2 - v^2\big)\big\}, \\
\frac{dv}{dt} &= -Su + \mu\big\{Av - (Bv - Cu)\big(u^2 + v^2\big) \\
&\quad + H_1\big(u^2 - v^2\big) + 2H_2 uv\big\}
\end{aligned} \tag{11}$$

where $u = r\cos\theta$, $v = -r\sin\theta$. Notice that the double perturbation procedure has been successfully applied in previous works to capture the dynamic in quasiperiodic Mathieu equations [15–18]. We rewrite (11) in the form

$$\begin{aligned}
\frac{du}{dt} &= Sv + \mu f(u, v), \\
\frac{dv}{dt} &= -Su + \mu g(u, v)
\end{aligned} \tag{12}$$

Using the multiple scales method, we expand the solutions of (12) as

$$\begin{aligned}
u(t) &= u_0(T_0, T_1, T_2) + \mu u_1(T_0, T_1, T_2) \\
&\quad + \mu^2 u_2(T_0, T_1, T_2) + O\big(\mu^3\big), \\
v(t) &= v_0(T_0, T_1, T_2) + \mu v_1(T_0, T_1, T_2) \\
&\quad + \mu^2 v_2(T_0, T_1, T_2) + O\big(\mu^3\big)
\end{aligned} \tag{13}$$

where $T_i = \mu^i t$. Substituting (13) into (12) and collecting terms, we get

– Order μ^0:

$$\begin{cases}
D_0^2 u_0 + S^2 u_0 = 0, \\
Sv_0 = D_0 u_0
\end{cases} \tag{14}$$

– Order μ^1:

$$\begin{cases}
D_0^2 u_1 + S^2 u_1 = -2D_0 D_1 u_0 + D_0(f(u_0, v_0)) \\
\qquad\qquad + Sg(u_0, v_0), \\
Sv_1 = D_0 u_1 + D_1 u_0 - f(u_0, v_0)
\end{cases} \tag{15}$$

– Order μ^2:

$$\begin{cases}
D_0^2 u_2 + S^2 u_2 = -2D_0 D_2 u_0 - D_0 D_1 u_1 \\
\qquad\qquad - SD_1 v_1 \\
\qquad\qquad + D_0\big(u_1 \frac{\partial f}{\partial u}(u_0, v_0) \\
\qquad\qquad + v_1 \frac{\partial f}{\partial v}(u_0, v_0)\big) \\
\qquad\qquad + S\big(u_1 \frac{\partial g}{\partial u}(u_0, v_0) \\
\qquad\qquad + v_1 \frac{\partial g}{\partial v}(u_0, v_0)\big), \\
Sv_2 = D_0 u_2 + D_1 u_1 + D_2 u_0 - \big(u_1 \frac{\partial f}{\partial u}(u_0, v_0) \\
\qquad + v_1 \frac{\partial f}{\partial v}(u_0, v_0)\big)
\end{cases} \tag{16}$$

where $D_i^j = \frac{\partial^j}{\partial T_i^j}$. A solution to the first order is given by

$$u_0(T_0, T_1) = R(T_1)\cos(ST_0 + \varphi(T_1)),$$
$$v_0(T_0, T_1) = -R(T_1)\sin(ST_0 + \varphi(T_1)) \tag{17}$$

Substituting (17) into (15), removing secular terms and using the expressions $\frac{dR}{dt} = \mu D_1 R + O(\mu^2)$ and $\frac{d\varphi}{dt} = \mu D_1 \varphi + O(\mu^2)$, we obtain the following *slow slow* flow system on R and φ:

$$\frac{dR}{dt} = AR - BR^3,$$
$$\frac{d\varphi}{dt} = -CR^2 \tag{18}$$

Then, the first-order approximate periodic solution of the slow flow (12) is given by

$$u(t) = R\cos \nu t,$$
$$v(t) = -R\sin \nu t \tag{19}$$

where the amplitude R and the frequency ν are obtained by setting $\frac{dR}{dt} = 0$ and given, respectively, by

$$R = \sqrt{\frac{A}{B}}, \tag{20}$$

$$\nu = S - CR^2 \tag{21}$$

Using (19), the modulated amplitude of quasiperiodic solution of (1), is approximated by

$$r(t) = \sqrt{u^2(t) + v^2(t)} = R \tag{22}$$

This indicates that the quasiperiodic modulation area is reduced, at this first-order approximation, to the unique curve given by

$$r_{\min} = r_{\max} = R \tag{23}$$

where $r_{\min}$ and $r_{\max}$ are the maximum and the minimum of the amplitude modulation, respectively. In Fig. 2 is plotted the amplitude-frequency response curve as well as the quasiperiodic modulation domain obtained numerically (double circles connected with a vertical line). The horizontal line lying in the middle of circles is the first-order approximation of the modulation amplitude to the slow flow limit cycle as given by (22). Since the frequency of this limit cycle must be positive, the condition $\nu \geq 0$ from (21) imposes this line to end at a certain value of the frequency ω corresponding to the limit $\nu = 0$. This is consistent with numerical integration because at this limit the amplitude of the limit cycle hits the subharmonic response curve and disappears via a heteroclinic connection. Notice that the first-order approximation fails to capture the quasiperiodic modulation domain (double circles).

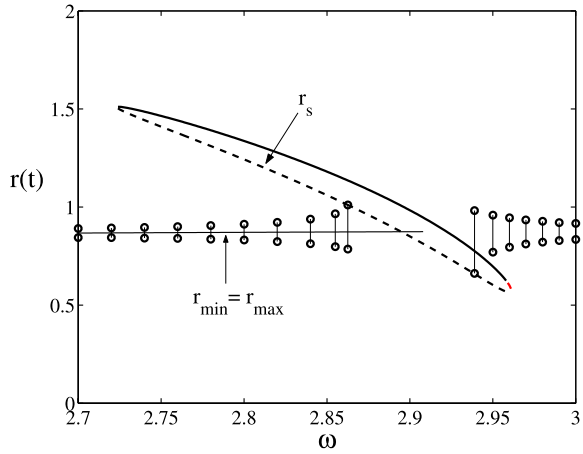

Fig. 2 Amplitude–frequency response curve and modulation amplitude of slow flow limit cycle. Numeric: *double circles*, analytic to the first order: *horizontal line*. Values of parameters are fixed as in Fig. 1

At the second-order approximations, a particular solution of system (15) is given by

$$u_1(T_0, T_1, T_2) = \frac{R^2(T_1, T_2)}{3S}(H_1\cos(2ST_0 + 2\varphi(T_1, T_2)) - H_2\sin(2ST_0 + 2\varphi(T_1, T_2))),$$
$$v_1(T_0, T_1, T_2) = \frac{R^2(T_1, T_2)}{3S}(H_1\sin(2ST_0 + 2\varphi(T_1, T_2)) + H_2\cos(2ST_0 + 2\varphi(T_1, T_2))) \tag{24}$$

Substituting (17), (18) and (24) into (16) and removing secular terms gives the following partial differential equations on R and φ:

$$D_2 R = 0,$$
$$D_2\varphi = -\frac{2R^2}{3S}\left(H_1^2 + H_2^2\right) \tag{25}$$

Then, the second-order approximate periodic solution of the slow flow (12) is now given by

$$u(t) = R\cos\nu t + \frac{R^2}{3S}(H_1\cos(2\nu t) - H_2\sin(2\nu t)),$$
$$v(t) = -R\sin\nu t + \frac{R^2}{3S}(H_1\sin(2\nu t) + H_2\cos(2\nu t) \tag{26}$$

where the amplitude R and the frequency ν are now obtained by setting $\frac{dR}{dt} = D_1 R + D_2 R = 0$ and given, respectively, by

$$R = \sqrt{\frac{A}{B}}, \tag{27}$$

$$\nu = S - \left(C + \frac{2R^2}{3S}\left(H_1^2 + H_2^2\right)\right)R^2 \tag{28}$$

Using (26), the modulated amplitude of quasiperiodic solution is now approximated by

$$r(t) = \sqrt{R^2 + \frac{R^4}{9S^2}\left(H_1^2 + H_2^2\right) + \frac{2R^3}{3S}(H_1\cos(3\nu t) - H_2\sin(3\nu t))} \tag{29}$$

Thus, the envelope of this modulated amplitude is delimited by $r_{\min}$ and $r_{\max}$ given by

$$r_{\min} = \sqrt{R^2 + \frac{R^4}{9S^2}\left(H_1^2 + H_2^2\right) - \frac{2R^3}{3S}\sqrt{H_1^2 + H_2^2}}, \tag{30}$$

$$r_{\max} = \sqrt{R^2 + \frac{R^4}{9S^2}\left(H_1^2 + H_2^2\right) + \frac{2R^3}{3S}\sqrt{H_1^2 + H_2^2}} \tag{31}$$

In Fig. 3 is plotted the modulated amplitude of slow flow limit cycle (solid lines), as given by (30), (31). The comparison between this analytical prediction and the numerical simulations (circles) indicates that the second-order analytical approximation can capture the modulation domain. Figure 3 shows that outside the synchronization area, quasiperiodic behavior takes place. When approaching the synchronization area, the upper limit of the modulation amplitude collides with the unstable frequency response curve producing a heteroclinic connection.

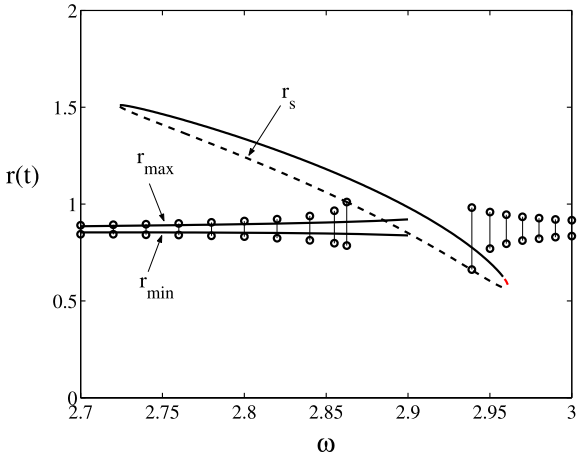

Fig. 3 Modulation amplitude of slow flow limit cycle. Numerical simulation: *double circles*, analytical approximation to the second order: *double lines*. Values of parameters are fixed as in Fig. 1

3 Collision criterion and heteroclinic bifurcation

An analytical approximation of the heteroclinic bifurcation curve is obtained by applying the collision criterion between the slow flow limit cycle and the three saddles. At the collision, this criterion may merely be given by the condition

$$r_{\max} = r_{\rm s} \tag{32}$$

where $r_{\max}$ is the upper limit of the modulation amplitude of the slow flow limit cycle given by (23) (first-order approximation) or by (31) (second-order approximation) and $r_{\rm s}$ denotes the amplitude of the unstable periodic orbit corresponding to the slow flow saddles obtained from the amplitude-frequency response (9). This analytical criterion of heteroclinic bifurcation is illustrated in Fig. 4 by the curves labeled H_a^1 (for the first order) and labeled H_a^2 (for the second order).

It is worth noticing that the condition $\nu = 0$ in (21), corresponding to infinite period of the slow flow limit cycle, offers another analytical criterion of heteroclinic connection, as was shown in previous works [8, 9].

To test the validity and the accuracy of the analytical prediction, we perform numerical simulations by integrating (11) using the Runge–Kutta method. The obtained numerical heteroclinic bifurcation curve, labeled H_n, is plotted in Fig. 4 for comparison with the analytical curves H_a^1 and H_a^2. It can be seen from this

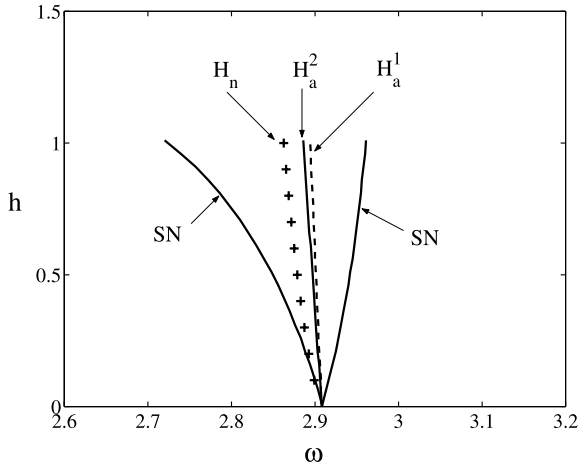

Fig. 4 Bifurcation curves for the 3:1 subharmonic resonance. *SN*: saddle-node bifurcation, H_a^1: analytical heteroclinic bifurcation curve to first order, H_a^2: analytical heteroclinic bifurcation curve to second order, H_n: numerical heteroclinic bifurcation curve. The values of parameters are fixed as in Fig. 1

comparison that for small values of the amplitude excitation h, the curves $H_a^{1,2}$ and H_n come closer.

In Table 1, we compare the values of the frequency ω corresponding to heteroclinic connection obtained by analytical predictions $\omega_a^{1,2}$ picked from H_a^1 and H_a^2, respectively, and through numerical calculation ω_n picked from H_n. Note that the curves labeled *SN* denote the saddle-node bifurcation locations for the 3:1 subharmonic cycles.

Figure 5 illustrates examples of phase portraits of the slow flow (11) for some values of ω picked from Fig. 3. For small values of ω, a slow flow limit cycle born by Hopf bifurcation exists and attracts all initial conditions. The related phase portraits are shown in subfigure (a) for $\omega = 2.72$. The subfigure (b) for $\omega = 2.80$ indicates the coexistence of a stable periodic orbit (stable equilibrium born by saddle-node bifurcation) and quasiperiodic (stable limit cycle) responses. As the forcing frequency varies, the stable slow flow limit cycle approaches the saddles and disappears via a heteroclinic bifurcation. The corresponding phase portrait is shown in subfigure (c) for the value $\omega = 2.86256$. This mechanism gives rise to frequency-locking, in which the response of the system follows the 3:1 subharmonic frequency (see subfigure (d) for $\omega = 2.90$).

We point out that in this study, we have focused on the heteroclinic bifurcation corresponding to the case where the limit cycle disappears leaving the cycles located outside the *triangle* connection, as shown in Fig. 5b, c. The other case of heteroclinic bifurcation leaving the cycles inside the *three-leaved clover* connection is not considered here. The phase portraits corresponding to this bifurcation are illustrated in Fig. 5e, f. Indeed, analytical analysis of the latter bifurcation requires an approximation of the slow flow limit cycle near the corresponding connection (Fig. 5f), which is not an easy task. Moreover, the phase portraits indicate that the frequency-locking occurs in a very small region of the frequency range ω, lying approximatively in the interval $2.863 \leq \omega \leq 2.939$.

Table 1 Comparison between analytical predictions (ω_a^1 for the first order, ω_a^2 for the second order) and numerical calculation (ω_n) of heteroclinic bifurcation, for different values of h. Values of parameters are fixed as in Fig. 1

	ω_a^1	ω_a^2	ω_n
$h = 1$	2.894	2.886	2.863
$h = 0.5$	2.901	2.897	2.879
$h = 0.1$	2.907	2.906	2.899

4 Conclusion

We have proposed an analytical approach to approximate bifurcation to heteroclinic cycles in a forced van der Pol–Duffing oscillator near the 3:1 resonance. This approach is based on the collision criterion between the slow flow limit cycle and the three saddles involved in the bifurcation. A second-order approximation of the criterion was performed using trigonometric functions in the construction of the limit cycle. A comparison to numerical simulations shown a satisfactory agreement indicating that the collision criterion can capture the heteroclinic bifurcation near the 3:1 subharmonic resonance. It should be emphasized that analytical approximation of heteroclinic bifurcation of cycles can be ameliorated by using higher order approximations.

We have focused our efforts on the heteroclinic bifurcation in the case where the limit cycle disappears leaving the cycles outside the *triangle* connection. To capture the heteroclinic bifurcation in the case when it leaves the cycles inside the *clover* connection, more efforts are required in term of approximating the slow flow limit cycle in the vicinity of this heteroclinic connection (see Fig. 5f).

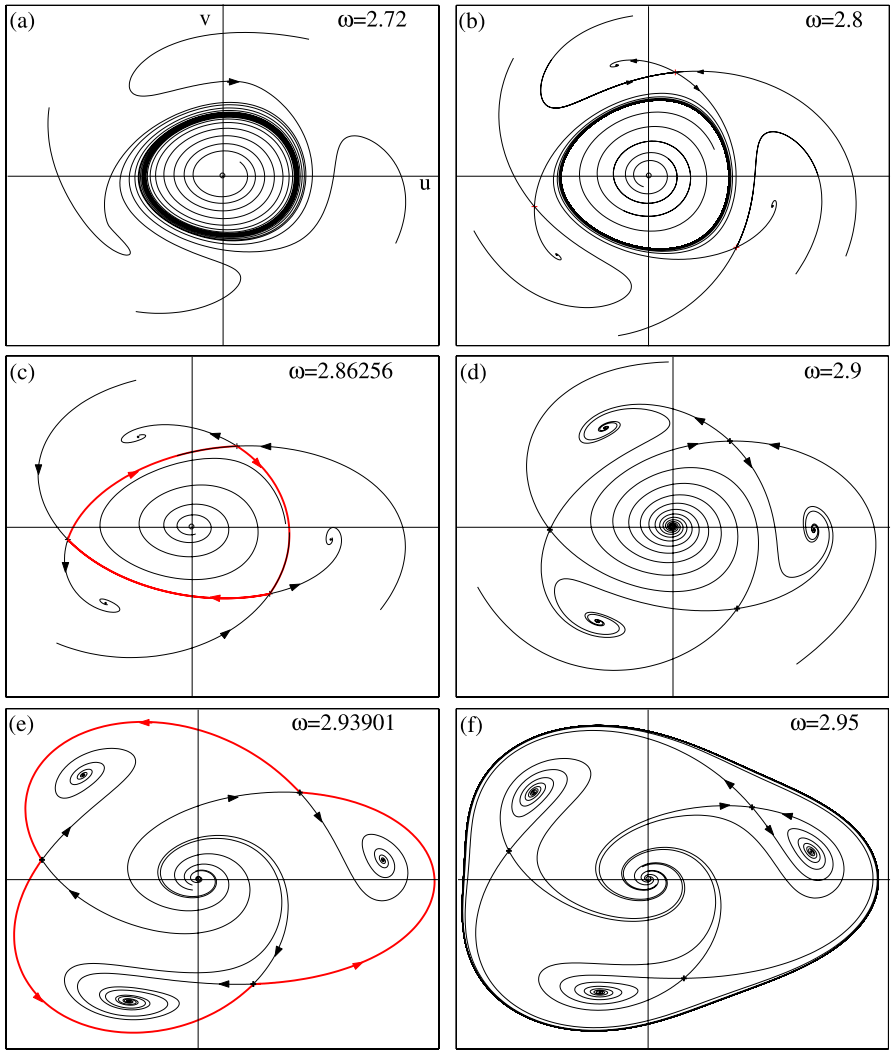

Fig. 5 Examples of phase portraits of the slow flow at different frequencies picked from Fig. 3. (**c**) *triangle* connection, (**e**) *clover* connection. Values of parameters are fixed as in Fig. 1

The idea of the present work combining the collision criterion with the Jacobian elliptic functions would significantly enhance the accuracy of the heteroclinic bifurcation approximation or even give a result equivalent to the Melnikov approach, if it is applied, as shown in [10]. The challenge here is to construct analytically the heteroclinic cycle and the slow flow limit cycle in its vicinity using the elliptic functions.

References

1. Belhaq, M., Clerc, R.L., Hartmann, C.: Étude numérique d'une 4-résonance d'une équation de Liénard forcée. C. R. Acad. Paris **303**(II9), 873–876 (1986) (in French)
2. Belhaq, M.: 4-subharmonic bifurcation and homoclinic transition near resonance point in nonlinear parametric oscillator. Mech. Res. Commun. **19**, 279–287 (1992)
3. Krauskopf, B.: On the 1:4 resonance problem. Ph.D. thesis, University of Groningen (1995)
4. Ashwin, P., Burylko, O., Maistrenko, Y.: Bifurcation to heteroclinic cycles and sensitivity in three and four coupled phase oscillators. Physica D **237**, 454–466 (2008)
5. Wiesenfeld, K., Colet, P., Strogatz, S.H.: Frequency locking in n Josephson arrays: connection with the Kuramoto model. Phys. Rev. E **57**, 1563–1569 (1998)
6. Viktorov, E.A., Vladimirov, A.G., Mandel, P.: Symmetry breaking and dynamical independence in a multimode laser. Phys. Rev. E **62**, 6312–6317 (2000)
7. Brown, E., Holmes, P., Moehlis, J.: Globally coupled oscillator networks. In: Kaplan, E., Marsden, J., Sreenivasan, K. (eds.) Perspectives and Problems in Nonlinear Science: A Celebratory Volume in Honor of Larry Sirovich, pp. 183–215. Springer, New York (2003)

8. Belhaq, M., Fahsi, A.: Homoclinic bifurcations in self-excited oscillators. Mech. Res. Commun. **23**, 381–386 (1996)
9. Belhaq, M., Lakrad, F., Fahsi, A.: Predicting homoclinic bifurcations in planar autonomous systems. Nonlinear Dyn. **18**, 303–310 (1999)
10. Belhaq, M., Fiedler, B., Lakrad, F.: Homoclinic connections in strongly self-excited nonlinear oscillators: the Melnikov function and the elliptic Lindstedt–Poincaré method. Nonlinear Dyn. **23**, 67–86 (2000)
11. Belhaq, M., Houssni, M., Freire, E., Rodriguez-Luis, A.J.: Asymptotics of homoclinic bifurcation in a three-dimensional system. Nonlinear Dyn. **2**, 135–155 (2000)
12. Belhaq, M., Lakrad, F.: Analytics of homoclinic bifurcations in three-dimensional systems. Int. J. Bifur. Chaos **12**, 2479–2486 (2000)
13. Belhaq, M., Fahsi, A.: Hysteresis suppression for primary and subharmonic 3:1 resonances using fast excitation. Nonlinear Dyn. **57**(1–2), 275–287 (2009)
14. Fahsi, A., Belhaq, M.: Hysteresis suppression and synchronization near 3:1 subharmonic resonance. Chaos Solitons Fractals **42**(2), 1031–1036 (2009)
15. Belhaq, M., Houssni, M.: Quasi-periodic oscillations, chaos and suppression of chaos in a nonlinear oscillator driven by parametric and external excitations. Nonlinear Dyn. **18**, 1–24 (1999)
16. Belhaq, M., Guennoun, K., Houssni, M.: Asymptotic solutions for a damped non-linear quasi-periodic Mathieu equation. Int. J. Non-Linear Mech. **37**, 445–460 (2000)
17. Rand, R., Guennoun, K., Belhaq, M.: 2:2:1 Resonance in the quasiperiodic Mathieu equation. Nonlinear Dyn. **31**, 367–374 (2003)
18. Abouhazim, N., Belhaq, M., Lakrad, F.: Three-period quasi-periodic solutions in the self-excited quasi-periodic Mathieu oscillator. Nonlinear Dyn. **39**, 395–409 (2005)
19. Nayfeh, A.H., Mook, D.T.: Nonlinear Oscillations. Wiley, New York (1979)